

A hot and luminous source at the site of the fast transient AT2018cow at 2–3 years after its explosion

Ning-Chen Sun^{1*}, Justyn R. Maund¹, Paul A. Crowther¹ and Liang-Duan Liu²

¹ Department of Physics and Astronomy, University of Sheffield, Hicks Building, Hounsfield Road, Sheffield S3 7RH, UK

² College of Physical Science and Technology, Central China Normal University, 152 Luoyu Road, Wuhan, Hubei 43079, China

Accepted XXX. Received YYY; in original form ZZZ

ABSTRACT

We report the discovery of a luminous late-time source at the position of the fast blue optical transient (FBOT) AT2018cow on images taken by the Hubble Space Telescope (HST) at 714 d and 1136 d after its explosion. This source is detected at both UV and optical wavelengths and has prominent H α emission. It has a very stable brightness between the two epochs and a very blue spectral energy distribution (SED) consistent with $f_{\lambda} \propto \lambda^{-4.1 \pm 0.1}$, i.e. the Rayleigh-Jeans tail of a hot blackbody with a very high temperature of $\log(T/K) > 4.6$ and luminosity of $\log(L/L_{\odot}) > 7.0$. This late-time source is unlikely to be an unrelated object in chance alignment, or due to a light echo of AT2018cow. Other possible scenarios also have some difficulties in explaining this late-time source, including companion star(s), star cluster, the survived progenitor star, interaction with circumstellar medium (CSM), magnetar, or delayed accretion in a tidal disruption event (TDE). Long-term and multi-wavelength monitoring will help to resolve its nature and finally reveal the origin of the ‘‘Cow’’.

Key words: stars: massive; supernovae: general; supernovae: individual: AT2018cow

1 INTRODUCTION

FBOTs have peak brightnesses comparable to those of (typical or superluminous) supernovae (SNe). As implied by their name, however, they exhibit very blue colors and evolve with much shorter timescales (Ho et al. 2021). Their rapid evolution is hard to explain with radioactive decay that powers most SNe, suggesting that they are a distinct new type of transients (e.g. Xiang et al. 2021, hereafter X21). At a distance of only 63 Mpc, AT2018cow is the closest FBOT ever discovered. It has a peak luminosity of $\sim 10^{44}$ erg s⁻¹, rises to peak in just a few days and then declines dramatically (Prentice et al. 2018; Perley et al. 2019, hereafter P19; Xiang et al. 2021). The photospheric temperature is $\sim 30,000$ K near peak and still as high as $\sim 10,000$ K at ~ 50 d after explosion (Kuin et al. 2019; P19; X21).

It is still unclear what progenitor is responsible for AT2018cow and what process(es) powers its rapid evolution. Current models include TDE (Liu et al. 2018; Kuin et al. 2019; P19), CSM interaction (Fox & Smith 2019; X21), magnetar (Prentice et al. 2018; Fang et al. 2019), pulsational pair-instability SN (PPISN; Leung et al. 2020), jet-envelope interaction in a core-collapse SN (Gottlieb, Tchekhovskoy, & Margutti 2022), or a jet-driven SN impostor from a common-envelope binary system (Soker 2022). It is worth mentioning that AT2018cow is located in an environment typical for core-collapse SNe (Lyman et al. 2020); more recently, Pasham et al. (2021) found evidence for a rapidly spinning compact object, which could be a neutron star or a black hole of mass $< 850 M_{\odot}$.

For a number of SNe, late-time observations sometimes reveal significant brightness unexpected from their early-time evolution.

The late-time sources contain important information for these SNe as their possible light echos (e.g. SN 2011dh; Maund 2019), binary companions (e.g. SN 1993J and SN 2006jc; Maund et al. 2004, 2016; Sun et al. 2020), host star clusters (e.g. SN 2014C; Sun, Maund, & Crowther 2020), late CSM interaction (e.g. SN 1993J; Zhang et al. 2004) or something else. In comparison, no late-time sources have ever been reported for FBOTs, most of which are located in distant galaxies and observations become very difficult beyond several months after their explosions.

Thanks to its relative proximity, AT2018cow may be the only possible FBOT to study its brightness at significantly late times. In this paper, we report the discovery of a bright source at the position of AT2018cow at 2–3 years after its explosion. This is somewhat surprising for a fast evolving transient with a steeply declining light curve. We describe the observed features and then discuss its possible origin scenarios.

Throughout this paper, we use a redshift of 0.01406 and a distance of 63 Mpc for the host galaxy (CGCG 137-068; X21) and a Galactic reddening of $E(B - V) = 0.078$ mag for AT2018cow (Schlafly & Finkbeiner 2011). Its internal reddening within the host galaxy is negligible (P19; X21). All epochs are relative to an estimated explosion date of MJD = 58,284.79 (X21).

2 DATA

AT2018cow was observed by three HST programs (Table 1), all conducted with the Ultraviolet-Visible (UVIS) channel of the Wide Field Camera 3 (WFC3). The first program (ID: GO-15600) was performed at $t = 52, 57$ and 62 d while the other two programs

* E-mail: n.sun@sheffield.ac.uk

Table 1. HST/WFC3/UVIS observations of AT2018cow.

Program ID	Epoch ^d (day)	Filter	Exposure Time (s)	Magnitude ^e (mag)
15600 ^a	52	F218W	880	19.12 (0.02)
	52	F225W	770	18.99 (0.01)
	52	F275W	280	18.88 (0.02)
	52	F336W	150	19.17 (0.02)
15600	57	F218W	880	19.58 (0.01)
	57	F225W	770	19.48 (0.01)
	57	F275W	280	19.34 (0.01)
	57	F336W	150	19.58 (0.01)
15600	62	F218W	880	19.75 (0.03)
	62	F225W	770	19.56 (0.01)
	62	F275W	280	19.56 (0.02)
	62	F336W	150	19.82 (0.02)
15974 ^b	714	F657N	1119	>24.65 (5 σ)
	714	F665N	1119	24.47 (0.24)
	714	F225W	1116	22.55 (0.06)
	714	F336W	1116	23.32 (0.05)
	714	F555W	1044	25.64 (0.07)
	714	F814W	1044	25.82 (0.19)
16179 ^c	1136	F555W	710	25.63 (0.08)
	1136	F814W	780	25.96 (0.24)

PIs: (a) Foley R.; (b) Levan A.; (c) Filippenko A.

(d) Epoch is relative to an explosion date of MJD = 58,284.79 (X21).

(e) All magnitudes are in the Vega system.

(IDs: 15974 and 16179) were carried out at significantly later times of $t = 714$ and 1136 d, respectively. We retrieved the images from the Mikulski Archive for Space Telescopes (<https://archive.stsci.edu/index.html>) and re-drizzled them with `driz_cr_grow = 3` for better cosmic ray removal (all other parameters were left unchanged as in the standard calibration pipeline).

In this work, we also use AT2018cow’s early-time light curves of P19 out to $t \gtrsim 60$ days. At optical wavelengths, the reported magnitudes in the Swift/UVOT and SDSS-like filters were converted into the Johnson-Cousins *UBVRI* system, using the relative offsets shown in Fig. 2 of P19. Magnitudes in the *V* and *I* bands are very similar to those in the F555W and F814W bands, respectively, with differences no larger than the photometric uncertainties (Harris 2018). Light curves in the Swift/UVOT UVM2 and UVW1 filters and in the *U* band were transformed to the HST F218W, F225W, F275W and F336W bands using relations derived with synthetic magnitudes of blackbody spectra of 7000–50,000 K (calculated with the `PYSYNPHOT` package). P19 used the AB magnitude system and we converted their magnitudes into the Vega magnitude system with $m_{\text{AB}} - m_{\text{Vega}} = 1.68, 1.66, 1.50, 1.19, -0.02$ and 0.43 mag for the F218W, F225W, F275W, F336W, F555W and F814W bands, respectively. These offsets were also calculated with the `PYSYNPHOT` package and are valid for hot sources like AT2018cow.

3 DETECTION OF A LATE-TIME SOURCE

We performed point-spread-function (PSF) photometry on the HST images with the `DOLPHOT` package (Dolphin 2000). At the position of AT2018cow, a point source is significantly detected in all the broadband images, only marginally detected in the F665N image with a 4.6σ significance, and not detected in the F657N image (Fig. 1). The

magnitudes or magnitude limits (obtained with artificial star tests) for this source are listed in the last column of Table 1. Note that the late-time source is not spatially resolved; therefore, its size should not significantly exceed that of the PSF, which corresponds to ~ 20 pc at the distance of AT2018cow.

Light curves At the first three epochs of the HST observations ($t = 52, 57$ and 62 d), the derived magnitudes are consistent with the light curves of P19 within the uncertainties (Fig. 2). AT2018cow’s brightness evolves very rapidly; if we simply extrapolate the light curve tails, the brightness should decline to a very low level within a few months. Somewhat surprisingly, there is still a bright source at the position of AT2018cow at $t = 714$ and 1136 d, or ~ 2 – 3 years after its explosion. It is also worth noting that the magnitudes of the late-time source are strikingly stable, in both F555W and F814W bands, over a time span of ~ 1.2 yr between the last two epochs. The magnitude differences are only 0.01 mag and 0.14 mag, respectively, much smaller than the photometric uncertainties.

SED The late-time source has an SED even bluer than AT2018cow at early times (Prentice et al. 2018; Kuin et al. 2019; P19; X21). In Fig. 3 the observed SED is compared with model spectra for blackbodies, single normal stars (Castelli & Kurucz 2004) and star clusters with a Salpeter (1955) initial mass function (IMF) from `BPASS` v2.1 binary population synthesis models (Eldridge et al. 2017). The late-time source has significant UV excess even compared with the hottest stars of $50,000 \text{ K}^1$ or the youngest star clusters of 1 Myr^2 . We find a power-law solution of $f_{\lambda} \propto \lambda^{-4.1 \pm 0.1}$ by fitting to the data, consistent with the Rayleigh-Jeans tail of very hot blackbodies.

Position on the HR diagram In Fig. 4 we show the possible positions of blackbodies on the HR diagram, whose synthetic magnitudes can match the observed ones for the late-time source. The result suggests that, if the late-time source is indeed a blackbody, it should have a very high temperature of $\log(T_{\text{eff}}/\text{K}) > 4.7$ and luminosity of $\log(L/L_{\odot}) > 7.0$, corresponding to a blackbody radius of several tens of solar radii. The derived luminosity is significantly higher than any typical single stars, which is obvious by comparing it with the Humphreys & Davidson (1979) limit³, the `PARSEC` single-stellar isochrones (Bressan et al. 2012), and some of the most luminous very massive stars of $>100 M_{\odot}$ in the Milky Way or in the Large Magellanic Cloud (Crowther et al. 2010; see also Bestenlehner et al. 2020). Note, however, that the bolometric luminosity remains very uncertain since it is not clear whether the late-time source deviates from a blackbody SED outside the observed wavelength range.

¹ If a star has strong wind, its continuum would appear redder and contamination due to emission lines is more significant for the optical filters than for the UV filters (Götberg, de Mink, & Groh 2017). Therefore, this effect is not able to explain the UV excess. We note, however, that the helium-burning Wolf-Rayet stars may reach significantly higher temperatures, up to 10^5 K (Crowther 2007), than the hottest stars included in the Castelli & Kurucz (2004) models.

² We also checked the effect of stochastic sampling on star clusters’ SEDs with the `SLUG` package (da Silva, Fumagalli, & Krumholz 2012; Krumholz et al. 2015). This effect may make the SEDs even redder, due to some massive stars having evolved into red supergiants, and thus more inconsistent with observations.

³ Recently, Davies, Crowther, & Beasor (2018) found evidence for an even lower luminosity limit for cool supergiants in the Magellanic Clouds.

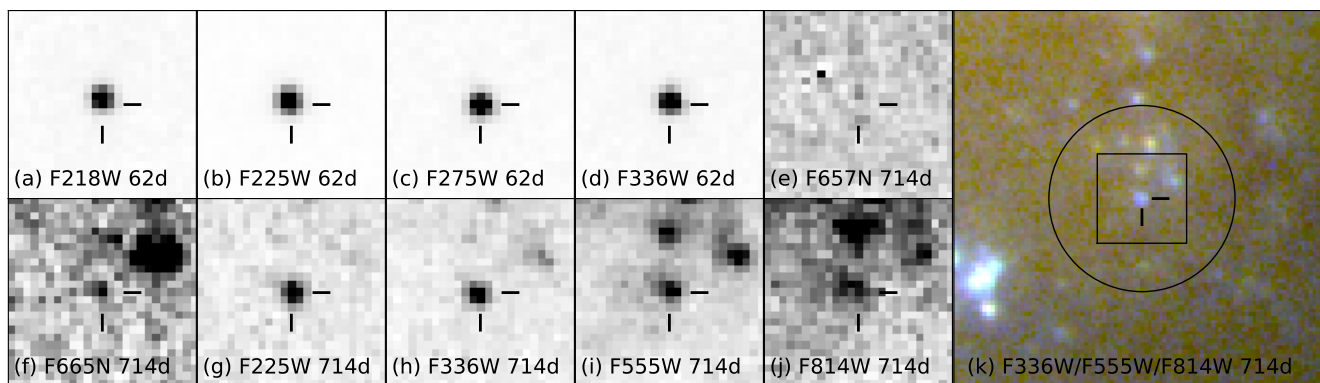


Figure 1. Example images of AT2018cow at early and late times of $t = 62$ d (a–d) and 714 d (e–j), respectively; each panel has a dimension of $1'' \times 1''$ and is centered on AT2018cow (shown by the cross hair). No source is detected at the position of AT2018cow in the F657N image (e). In the F814W image (j), the late-time source is not very obvious by eye due to a bright neighboring star to its northeast. (k) Three-color composite of the F336W, F555W and F814W images at $t = 714$ d; the square corresponds to the extent of the other panels (a–j) and the circle has a radius of $1''$. All panels are aligned with North up and East to the left. An angular size of $1''$ corresponds to a linear size of 305 pc at the distance of AT2018cow.

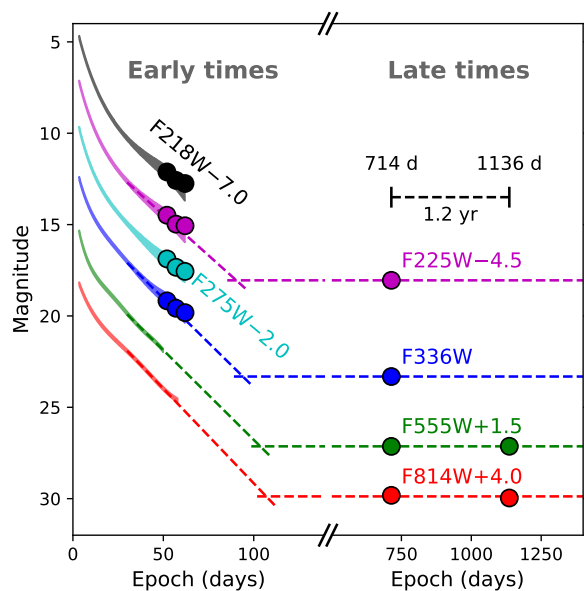


Figure 2. HST photometry of AT2018cow (filled circles) with error bars smaller than the symbol size. The solid lines are AT 2018cow’s early-time light curves reported by P19 (with line thickness showing the photometric uncertainties), which have been converted into the HST filters and the Vega magnitude system. The dashed lines correspond to linear extrapolations of the light curve tails or the brightness of the late-time source.

H α emission The F665N detection indicates prominent H α emission from the late-time source (Fig. 3). Note that the wavelength of H α is redshifted away from F657N into the F665N band due to the recession of the host galaxy. By subtracting a continuum interpolated between the F555W and F814W bands, we estimate a wavelength-integrated line flux of $\sim 10^{-17}$ erg s $^{-1}$ cm $^{-2}$ or an H α luminosity of $\sim 4 \times 10^{36}$ erg s $^{-1}$ (corrected for extinction). It is not clear whether the H α emission arise from stellar sources (e.g. WNh stars; Schaerer & Vacca 1998) and/or from a modest and compact H II region at the position of AT2018cow (for comparison, H II regions have H α luminosities ranging from 10^{37} erg s $^{-1}$ for the Orion Nebula to $>10^{40}$ erg s $^{-1}$ for 30 Doradus; Crowther 2013). With integral-field

spectroscopy, Lyman et al. (2020) found AT2018cow to be associated with a giant H II region. The F665N image, which has a much higher spatial resolution, shows that the giant H II region is actually to the northwest of AT2018cow with an offset of ~ 100 pc. Therefore, the detected F665N source is not due to the giant H II region in the environment of AT2018cow.

4 POSSIBLE ORIGINS

In this section we discuss what objects or physical mechanism(s) may give rise to the late-time brightness of AT2018cow.

Chance alignment The detected late-time source is less likely due to an unrelated object in chance alignment. We performed relative astrometry with 11 reference stars between the late-time images and the F218W image at $t = 62$ d. The (transformed) positions have an offset of only 0.3 pixel between AT2018cow and the late-time source, smaller than the astrometric uncertainty of 0.5 pixel. Additionally, there are only 22 sources significantly detected within $1''$ from AT2018cow (Fig. 1k); the probability is $<1\%$ for a randomly positioned source to coincide with AT2018cow within the 1σ error radius. Moreover, very few sources in the surrounding region can match AT2018cow’s late-time brightness and its very blue SED. Therefore, we suggest the late-time source is not in chance alignment but physically associated with AT2018cow.

Light echo It is very difficult to explain AT2018cow’s late-time brightness with a light echo. The H α emission is inconsistent with AT2018cow’s featureless spectrum near peak (P19; X21), and it may require a very specific dust configuration to reproduce its very blue SED. For circumstellar dust from a steady wind, the brightness of its light echo declines continuously (Chevalier 1986), inconsistent with the observed stable F555W/F814W brightness from $t = 714$ d to 1136 d. A foreground dust sheet may produce a stable light echo brightness if it is distant enough from the transient (Cappellaro et al. 2001). However, AT2018cow has a negligible amount of dust in its foreground since observations find very little extinction from within the host galaxy (P19; X21). For dust in the background, the scattering is much less efficient due to the large scattering angles (Draine 2003). Therefore, it seems unlikely that the late-time source is a light echo.

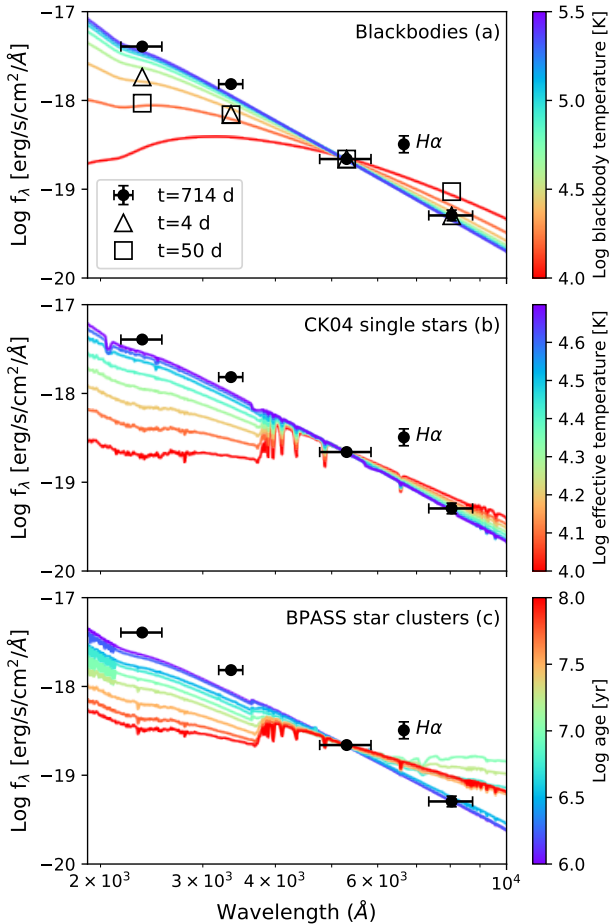


Figure 3. SED of AT2018cow’s late-time source (black data points); the horizontal error bars correspond to the root-mean-square widths of the HST filters and the vertical error bars reflect photometric uncertainties (if not smaller than the symbol size). The F657N detection limit does not provide additional constraint and is omitted in the plot. For comparison we show model spectra (colored lines) for (a) blackbodies, (b) single stars (Castelli & Kurucz 2004), and (c) star clusters (from BPASS v2.1 binary population synthesis; Eldridge et al. 2017), all reddened with AT2018cow’s Galactic reddening and normalized to the F555W band. In (a) we also show the early-time SED of AT2018cow at $t = 4$ d (open triangles) and 50 d (open squares) normalized to the F555W band; their error bars are no larger than the symbol size.

Stellar source(s) A late-time source with stable brightness is naturally expected if the transient’s progenitor is located inside a binary/multiple system (Maund et al. 2004, 2016; Sun et al. 2020, 2022) or star cluster (Sun, Maund, & Crowther 2020). For AT2018cow, the late-time source is inconsistent with a single companion star; the very high luminosity requires it to be at least 2–3 very massive ($>100 M_{\odot}$) stars inside a multiple system (Fig. 4). Star clusters with standard IMFs are difficult to match the observed SED (Fig. 3); if the late-time source were indeed a star cluster, it may have a very top-heavy IMF (e.g. Schneider et al. 2018) so that the brightness is dominated by the very massive stars.

It is unclear if FBOTs mark the death of massive stars or arise from their non-terminal explosions. In a PPISN, for example, material ejected at a later epoch may collide with earlier ejecta, producing a luminous transient, but the progenitor may not have completely

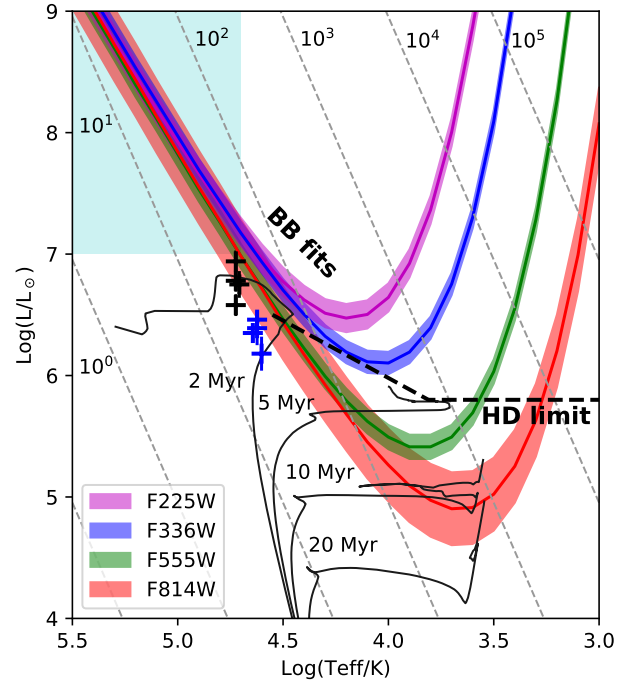


Figure 4. In this HR diagram, we use a color-shaded region, for each HST band, to show the possible positions of blackbodies whose synthetic magnitudes match the observed late-time brightness of AT2018cow within 5σ uncertainties. The four regions should converge together if the observed SED is indeed a blackbody spectrum across all four bands. This is met at $\log(T_{\text{eff}}/K) > 4.7$ and $\log(L/L_{\odot}) > 7.0$, i.e. the light blue-shaded area in the upper-left corner. The grey dashed lines correspond to constant blackbody radii and the labelled values are in units of solar radius (R_{\odot}). The thin black solid lines are PARSEC v1.2S single stellar isochrones (Bressan et al. 2012) and the thick black dashed line is the Humphreys & Davidson (1979) limit for stellar luminosity. The “+” symbols show some of the most luminous stars in the Milky Way (NGC 3603-A1a, A1b, B and C; in blue) and the Large Magellanic Cloud (R136a1–3 and b; in black; Crowther et al. 2010).

destroyed itself and can still be observed at late times (Woosley, Blinnikov, & Heger 2007). It is, however, still difficult to explain the high luminosity of AT2018cow’s late-time source unless the progenitor is overluminous due to some special mechanisms. In a PPISN model of AT2018cow, Leung et al. (2020) found a progenitor mass of $M_{\text{ini}} \sim 80 M_{\odot}$ in order to fit the fast evolving light curves.

In these scenarios, the $H\alpha$ emission may arise from stars with strong winds or from the local ionized gas, and AT2018cow is (probably) related to a very young and massive progenitor. Caution, however, that some SNe spatially aligned with young star clusters are found to have much older progenitors due to sequentially triggered star formation (e.g. SN 2012P; Sun et al. 2021).

Late emission from AT2018cow AT2018cow has been proposed to be a core-collapse SN powered by CSM interaction (Fox & Smith 2019, X21). In the model of X21, AT2018cow was surrounded by CSM with a flat density profile from 3 to $1200 R_{\odot}$. If the late-time source were also due to CSM interaction, then the CSM should extend out to a much larger distance of $\gtrsim 5 \times 10^{16}$ cm (for an ejecta velocity of 5000 km/s); the CSM density may also be different at larger distances in order to explain the significant light curve flattening from early to late times. In this scenario, the late-time emission may be contributed by emission lines. However, it may be challenging

to reproduce the very stable brightness from $t = 714$ to 1136 d; most interacting SNe have time-varying brightness and their light curve plateaus, if any, last for much shorter periods (Mauerhan et al. 2013a,b; but see Smith et al. 2009 for the exceptions of extremely enduring SN 1988Z and SN 2005ip).

In a magnetar-powered model of AT2018cow, Prentice et al. (2018) derived a spin period of 11 ms and a magnetic field strength of 2.0×10^{15} G, corresponding to a magnetic dipole spin-down timescale of 0.3 d (Fang et al. 2019). In this case, the energy injection rate is expected to decline by 60% from $t = 714$ d to 1136 d, inconsistent with the observed very stable late-time brightness.

AT2018cow has also been suggested to arise from a low-mass star disrupted by an intermediate-mass black hole (Liu et al. 2018; Kuin et al. 2019; P19). In such a TDE, the stellar debris is usually assumed to be swallowed within a few orbits, giving rise to a $t^{-5/3}$ declining light curve after peak (Rees 1988). We might expect some late-time brightness if there is significant time delay for some of the debris to be accreted. In this case, a constant accretion rate is needed to explain the stable F555W/F814W brightness at 714–1136 d; the $H\alpha$ detection also requires the disrupted star to be hydrogen-rich.

5 SUMMARY

In this paper we report the discovery of a late-time source of the FBOT AT2018cow at 714 d and 1136 d after its explosion. It has a very stable brightness between the two epochs and a very blue SED consistent with the Rayleigh-Jeans tail of a blackbody spectrum with temperature $\log(T/K) > 4.7$ and luminosity $\log(L/L_{\odot}) > 7.0$. Significant $H\alpha$ emission is also detected. This late-time source is unlikely an unrelated object in chance alignment, or due to a light echo of AT2018cow. We discussed other possible scenarios as stellar source(s) (companion stars, star cluster, or the survived progenitor star) or due to AT2018cow's late emission (CSM interaction, magnetar, or delayed accretion in a TDE). All these scenarios have some difficulties in explaining this late-time source and require some fine tuning or special mechanisms to match the observations. It cannot be ruled out, however, that the late-time brightness is contributed by multiple components and/or processes. We believe this late-time source may contain important information for AT2018cow, but long-term monitoring and multi-wavelength observations are required to resolve its origin.

ACKNOWLEDGEMENTS

We thank the anonymous referee for the very helpful comments on our paper. Research of N-CS and JRM is funded by the Science and Technology Facilities Council through grant ST/V000853/1. L-DL is supported by the National Key R&D Program of China (2021YFA0718500). This paper is based on observations made with the NASA/ESA Hubble Space Telescope and has used the light curves published by P19.

DATA AVAILABILITY

Data used in this work are all publicly available from the Mikulski Archive for Space Telescope (<https://archive.stsci.edu>) or from the paper by P19.

REFERENCES

- Bestenlehner J. M., et al., 2020, MNRAS, 499, 1918
 Bressan A., et al., 2012, MNRAS, 427, 127
 Cappellaro E., et al., 2001, ApJL, 549, L215
 Castelli F., Kurucz R. L., 2004, preprint (arXiv:astro-ph/0405087)
 Chevalier R. A., 1986, ApJ, 308, 225
 Crowther P. A., 2007, ARA&A, 45, 177
 Crowther P. A., Schnurr O., Hirschi R., Yusof N., Parker R. J., Goodwin S. P., Kassim H. A., 2010, MNRAS, 408, 731
 Crowther P. A., 2013, MNRAS, 428, 1927
 da Silva R. L., Fumagalli M., Krumholz M., 2012, ApJ, 745, 145
 Davies B., Crowther P. A., Beasor E. R., 2018, MNRAS, 478, 3138
 Dolphin A. E., 2000, PASP, 112, 1383
 Draine B. T., 2003, ApJ, 598, 1017
 Eldridge J. J., et al., 2017, PASA, 34, e058
 Fang K., Metzger B. D., Murase K., Bartos I., Kotera K., 2019, ApJ, 878, 34
 Fox O. D., Smith N., 2019, MNRAS, 488, 3772
 Göteborg Y., de Mink S. E., Groh J. H., 2017, A&A, 608, A11
 Gottlieb O., Tchekhovskoy A., Margutti R., 2022, arXiv, arXiv:2201.04636
 Harris W. E., 2018, AJ, 156, 296
 Ho A. Y. Q., et al., 2021, arXiv, arXiv:2105.08811
 Humphreys R. M., Davidson K., 1979, ApJ, 232, 409
 Krumholz M. R., Fumagalli M., da Silva R. L., Rendahl T., Parra J., 2015, MNRAS, 452, 1447
 Kuin N. P. M., et al., 2019, MNRAS, 487, 2505
 Lyman J. D., Galbany L., Sánchez S. F., Anderson J. P., Kuncarayakti H., Prieto J. L., 2020, MNRAS, 495, 992
 Leung S.-C., Blinnikov S., Nomoto K., Baklanov P., Sorokina E., Tolstov A., 2020, ApJ, 903, 66
 Liu L.-D., Zhang B., Wang L.-J., Dai Z.-G., 2018, ApJL, 868, L24
 Mauerhan J. C., et al., 2013, MNRAS, 430, 1801
 Mauerhan J. C., et al., 2013, MNRAS, 431, 2599
 Maund J. R., Smartt S. J., Kudritzki R. P., Podsiadlowski P., Gilmore G. F., 2004, Natur, 427, 129
 Maund J. R., Pastorello A., Mattila S., Itagaki K., Boles T., 2016, ApJ, 833, 128
 Maund J. R., 2019, ApJ, 883, 86
 Pasham D. R., et al., 2021, NatAs.tmp, 245
 Perley D. A., et al., 2019, MNRAS, 484, 1031
 Prentice S. J., et al., 2018, ApJL, 865, L3
 Rees M. J., 1988, Natur, 333, 523
 Salpeter E. E., 1955, ApJ, 121, 161
 Schaerer D., Vacca W. D., 1998, ApJ, 497, 618. doi:10.1086/305487
 Schlafly E. F., Finkbeiner D. P., 2011, ApJ, 737, 103
 Schneider F. R. N., et al., 2018, Sci, 359, 69
 Smith N., et al., 2009, ApJ, 695, 1334
 Soker N., 2022, arXiv, arXiv:2201.07728
 Sun N.-C., Maund J. R., Hirai R., Crowther P. A., Podsiadlowski P., 2020, MNRAS, 491, 6000
 Sun N.-C., Maund J. R., Crowther P. A., 2020, MNRAS, 497, 5118
 Sun N.-C., Maund J. R., Crowther P. A., Fang X., Zapartas E., 2021, MNRAS, 504, 2253
 Sun N.-C., et al., 2022, MNRAS, 510, 3701
 Woosley S. E., Blinnikov S., Heger A., 2007, Natur, 450, 390
 Xiang D., et al., 2021, ApJ, 910, 42
 Zhang T., et al., 2004, AJ, 128, 1857

This paper has been typeset from a $\text{\TeX}/\text{\LaTeX}$ file prepared by the author.